Chalcogenide Letters Vol. 6, No. 12, December 2009, p. 655 – 660

DIELECTRIC BEHAVIOR AND AC ELECTRICAL CONDUCTIVITY ANALYSIS OF ZnSe CHALCOGENIDE NANOPARTICLES

MOHD. SHAKIR[A,B], B. K. SINGH[C], R. K. GAUR[D], BINAY KUMAR[C], G. BHAGAVANNARAYANA[B], M.A. WAHAB[A*]

[a]*Crystal Growth Lab, Department of Physics, Jamia Millia Islamia, New Delhi – 110 025, India*

[b]*Materials Characterization Division, National Physical Laboratory, New Delhi – 110 012, India*

[c]*Crystal Lab, Department of Physics & Astrophysics, University of Delhi, Delhi– 110 007, India*

[d]*Advance Ceramic Lab, National Physical Laboratory, New Delhi –110 012, India*

Zinc Selenide nanoparticles were synthesized successfully by microwave heating process. The phase of the synthesized nanoparticle was confirmed by powder X-ray diffraction analysis. The homogeneity and morphology of the synthesized nanoparticles was confirmed by scanning electron microscopy study. Further, the crystallite size was calculated by Scherer formula and found 32 nm. The average particle size of the synthesized nanoparticles was measured and found 45 nm, which is in close approximation with each other. The temperature and frequency dependence of dielectric constant and ac electrical conductivity measurements of the synthesized nanoparticles were carried out for the first time. Few anomalies in dielectric studies were observed near 200 and 375 ^{o}C, respectively. These points were related to glass and amorphous to crystalline phase transitions, respectively. The variation of activation energy and conduction behavior has been studied in the vicinity of transition temperatures in the ac conductivity measurements.

(Received November 10, 2009; accepted December 11, 2009)

Keywords: Semiconductor, nanostructures, scanning electron microscopy, dielectric properties

1. Introduction

Zinc Selenide (ZnSe) is a promising candidate from II-VI semiconducting materials due to their potential application in optoelectronic devices such as green-blue light emitting diodes (LED), laser diodes (LD) and solar cell, etc. [1–3]. ZnSe is a direct band gap semiconductor material with energy band gap 2.8 eV at room temperature [4]. This makes it a promising material for photo-electronic devices. It can also be used as dielectric mirrors; optically controlled switching devices [5,6]. Therefore, ZnSe is of great interest as a model material in such form as thin film, quantum wells and bulk crystals [7]. Since last three decades the nanosize materials, as a type of new quantum solid materials, have been subjected to extensive research for their unique physical and chemical properties. A wide range of applications could be anticipated in the use of nanometer size particles in electronic devices [8].

In recent years, due to the number of practical applications in the field of optoelectronics and electro-optics, a great deal of interest has been shown in the study of the dielectric and conduction behavior of various semiconducting materials [9-12]. However, most of the experimental work carried out so far for ZnSe relates to various conduction mechanisms, which only provides information about the nature of transport processes. Despite the intense research on

ZnSe that have been carried out till date, the experimental results on dielectric study are very few, and that too are very less informative [13]. It is well known that dielectric properties of every solid are very sensitive to the local electric field distribution in the sample. Therefore, the temperature and frequency dependence of dielectric constant and loss can explore useful information about structure changes, transport mechanism and defect behavior.

In the present investigation, the synthesis of ZnSe nanoparticles (using Zn and Se elements) with homogeneous crystallite size using microwave heating process is achieved. The synthesized nanoparticles were subjected to powder XRD for the phase confirmation. The scanning electron microscopic study has been done to check the morphology and particle size of nanoparticles. The temperature dependence of dielectric constant, loss and ac conductivity were (range 30 ^{0}C to 600 ^{0}C) carried out in wide range of frequency (100 Hz - 2MHz). The results are analyzed and discussed in detail.

2. Experimental details

The synthesis of ZnSe has been done using high purity Zn and Se (99.99%, M/S Sigma Aldrich) taken in equimolar ratio by microwave heating process. About 25 gm of material in their stoichiometric ratio was taken and placed in a thoroughly cleaned high quality quartz ampoule (using acetone and dried in a furnace at 600 ^{0}C for 5 h) of dimension 15 cm length, 2cm inner diameter and 3mm wall thickness. The quartz ampoule containing the material in powder form was evacuated (upto 10^{-6} Torr) using a high vacuum system and then sealed. The sealed ampoule was placed in a microwave furnace with a power rating and operating frequency of 8.8 kW and 2.8 GHz, respectively. The ampoule was rocked continuously (without interrupting the heating) by a slow moving motor for proper redistribution. The content of the ampoule become reddish yellow hot indicating that quite a high temperature ~875 ^{0}C was reached within a short time. The complete synthesis of the materials was done within a short time ~ 30 min. After 30 min of synthesis, the material was in spongy form and turned yellow [14]. The yellow color of the material is also indicating the synthesis of title material.

The Powder X-ray diffraction analysis (PXRD) of the synthesized material was carried out by using PW3710 based Philips analytical powder X-ray diffractometer. The morphology and particle size analysis of the synthesized nanoparticle was carried out using scanning electron microscopy. The synthesized nanoparticles were regrind and mixed with binder (Polyvinyl Alcohol). The mixture was then heated at 300 ^{o}C to burnout the binder. Further, a pallet of 12 mm diameter and 1.2 mm thickness were made by applying 250 MPa of pressure using hydraulic press for further analysis. The prepared pallet was then used for dielectric measurement by coated its opposite faces using high grade conducting layer of Silver paste. The variation of dielectric constant (real and imaginary), loss and ac conductivity with temperature at different frequency (100 Hz-2MHz) was studied from room temperature to 600 ^{o}C using a Agilent E4980A impedance analyzer. For measurement, sample was placed in a computer controlled heating chamber (accuracy $\pm$ 1^{o}C) and the temperature was varied from 30 to 600 ^{o}C at the rate of 3^{o}C/min. The results were analyzed and discussed in detail.

3. Result and discussion

3.1 Powder X-ray diffraction analysis

The PXRD pattern for the synthesized ZnSe nanoparticles was recorded. The room temperature PXRD data is analyzed using "X'Pert HighScore Plus" and Chekcell software for calculating cell parameters and refining the obtained cell parameters, respectively. The refined values were found to be of cubic phase with cell parameter a=b=c=5.6613Å and α=β=γ=90^0, which is in good agreement with the earlier reported value [JCPDS-37-1463]. The crystallite size of the synthesized ZnSe nanoparticle was calculated using Scherer's formula $D = 0.9\lambda / \beta\cos\theta$;

where, D is the average crystallite size, λ is the X-ray wavelength (1.5405Å) and β is full width at half maximum in radian. The average crystallite size for (111) plane is found to be ~32 nm.

3.2 Scanning electron microscope

The uniformity, homogeneity and a sphere-like morphology is confirmed in SEM micrograph Fig.1. The average particle size of the synthesized ZnSe nanoparticles was measured and found to be ~45 nm, which is in good agreement with the powder XRD result.

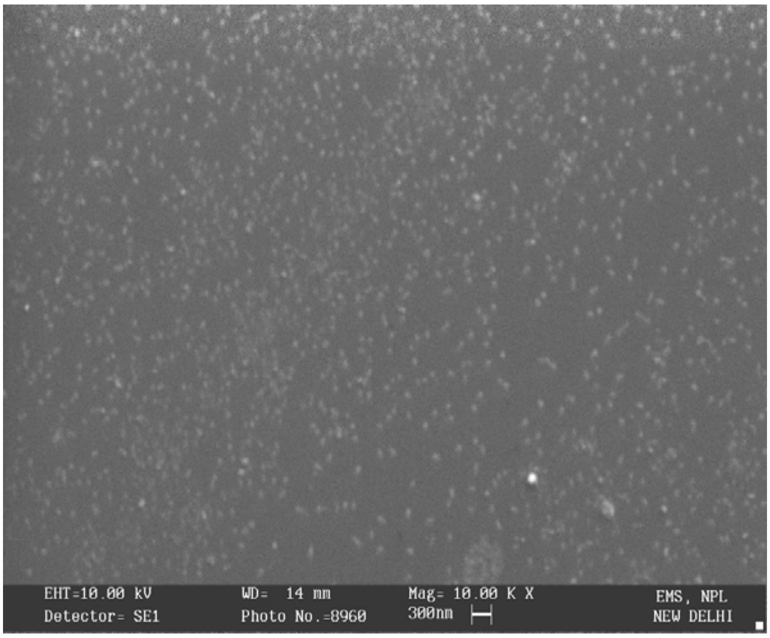

Fig. 1 SEM micrograph of ZnSe nanoparticles.

3.3 Dielectric Analysis

Dielectric studies of the prepared pallet of the synthesized ZnSe nanoparticles were carried out to analyze its response to an applied low ac voltage (1V). The variation of ε' with temperature at various frequencies is shown in Fig. 2(a). A dielectric constant as high as ~10^6 is observed at higher temperature. A broad dielectric peak near 200 ^{o}C is attributed to the glass transition temperature. A sharp peak at ~375 ^{o}C is observed at lower frequencies (upto 10 kHz). At first glance it is assumed to be sphalerite-type hexagonal phase transition of ZnSe. But, when the experiment is repeated no peak at 375 ^{o}C is observed. So, we attributed that this peak may be due to amorphous to crystalline transition. This shows that the as prepared sample contains amorphous as well as crystalline phase of ZnSe. The variation of the dissipation factor tan δ is as shown in Fig. 2(b). A nearly similar trend as that of dielectric constant with temperature is observed for dielectric loss [Fig. 2(b)]. A sharp rise in the tan δ is also observed from room temperature to 200 ^{o}C, which possibly may be due to increase in the ionization of the sample with temperature which increases the conductivity processes and dissipation factor simultaneously. A sharp dip at ~375 ^{o}C is may be due to transition from amorphous to crystalline state, which eventually decreases conductivity and hence dielectric loss.

The variation of the imaginary part of dielectric constant with frequency is shown in Fig. 2(c). Jonscher [15] suggested that the behavior of dipolar system can be characterized by fractional power laws in frequency above the loss peak frequency as $\varepsilon'' \propto f^{n-1}$, where (0<n<1). After fitting the curve the exponent n is found to increase from 0.13 to 0.24 as temperature increases from 30 to 600 ^{o}C.

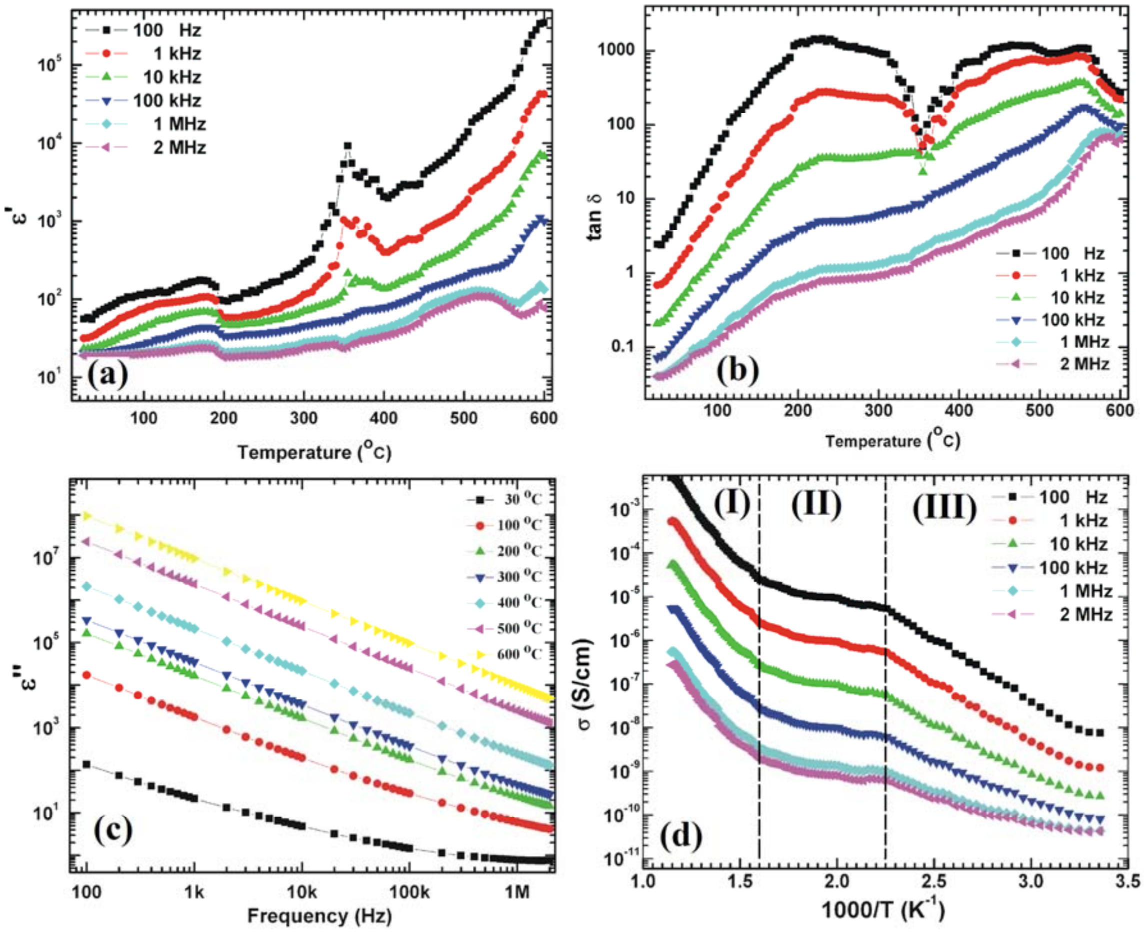

Fig. 2 Variation of (a) real part of dielectric constant (b) dielectric loss with temperature at various frequencies (c) imaginary part of dielectric constant with frequency at different temperatures (d) ac conductivity with inverse of temperature at different frequencies.

3.4 AC Conductivity

The ac conductivity σ can be directly related to the imaginary part of dielectric constant (ε'') as $\sigma = \varepsilon_o \omega \varepsilon''$ Where, ε_o and ω is permittivity of free space and angular frequency, respectively. The variation of ac conductivity with temperature is shown in Fig. 2(d). A smooth increase in the ac conductivity is observed throughout the temperature range. However, an anomaly is observed near 170 °C which may be due to glass transition temperature. A nearly invariant temperature dependence of ac conductivity is seen in the temperature range 170-300 °C, beyond which a sharp increase at 300 °C is observed. The activation energy for conduction (E_a) in the entire region as shown in Fig. 3(a) for various frequencies was calculated by fitting different regions with the equation $\sigma_{ac} = \sigma_o e^{-E_a/k_B T}$. The variation of the activation energy with frequency for all the three regions is shown in Fig. 3a. The activation energy is found to decrease with increasing frequency.

The ionic conductivity can be related to diffusion constant (D) using Einstein relation [16] as $\sigma / D = Ne^2 / k_B T$. This relation can be extended further as $n(k_B T\varepsilon'') = \ln(Ne^2 D_0 / \varepsilon_0) - \ln(\omega) - (E_t / k_B T)$, Where, D_o, E_t is the maximum diffusion coefficient and total activation energy due to bulk and surface conduction, respectively [17]. From this equation it is evident that a plot between $\ln(k_B T\varepsilon'')$ and $1/T$ will give a straight line whose slope will represent E_t / k_B. The variation of $\ln(k_B T\varepsilon'')$ with $1000/T$ is shown in Fig. 3(b). A similar trend as of ac conductivity is observed. The complete temperature region for the plot can be divided into three regions, in which it responds differently. In the first region a linear increase is observed with a peak at nearly 175 ^{o}C (glass transition temperature). Further, in the temperature range 170-300 ^{o}C a nearly invariant response to the temperature is observed, similar to ac conductivity. However, a sharp increase in $\ln(k_B T\varepsilon'')$ beyond 300 ^{o}C is observed. The variation of $\ln(k_B T\varepsilon'')$ for all the three regions for various frequencies is subjected to linear fitting to calculate the totals activation energy for conduction (due to bulk and surface conduction). The variation of E_t with frequency is shown in Fig. 3(c).

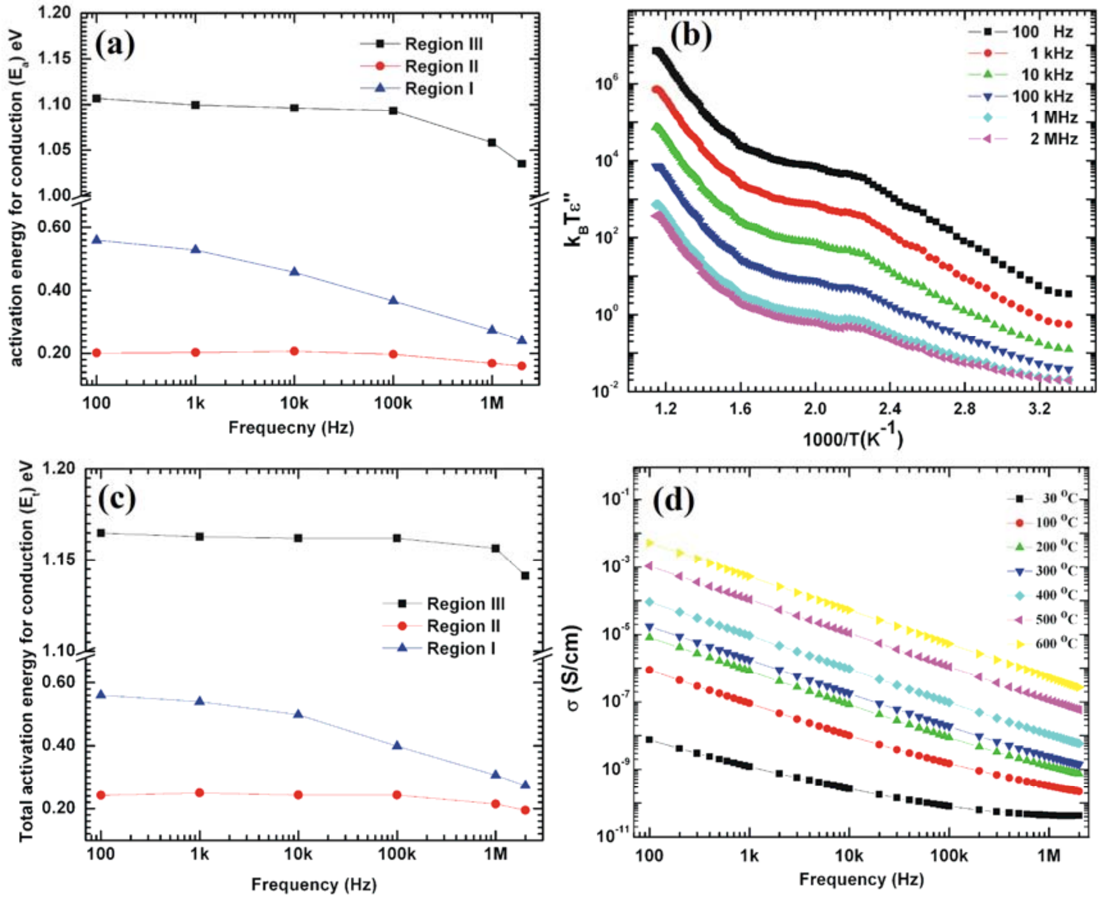

Fig. 3 Variation of (a) activation energy for conduction with frequency in different regions (b) $\ln(k_B T\varepsilon'')$ with 1000/T (c) total activation energy for conduction with frequency in different regions and (d) ac conductivity with frequency at different temperature.

Fig. 3d shows the variation of ac conductivity with frequency. A sharp decrease in σ is observed upto 2 MHz. The frequency dependence of σ is analyzed using power square law given by Jonscher, the conductivity follows the Jonscher power law relation $\sigma = A\omega^s$, where ω is the angular frequency, '*A*' is a constant and the exponent '*s*' is a frequency-dependent parameter having values less than unity [18]. The value of exponent 's' at different temperature is calculated by fitting the curve Fig. 3(d) and found to increase from 0.23 to 0.41 when temperature increases from 30 to 600 ^{o}C.

4. Conclusions

ZnSe nanoparticles were synthesized within a short time. The confirmation of the present phase and stiochiometery of synthesized nanoparticles was studied by using powder X-ray diffraction. The SEM study reveals the synthesized particles are homogeneous with sphere like morphology. The measured average particle size and calculated crystallite size was calculated and found to be ~45 and ~32 nm, respectively. In the dielectric studies the phase transitions at 200 and 375 ^{0}C was observed which may be due to the glass phase transition and amorphous to crystalline nature of the synthesized material. This shows that the as prepared sample contains amorphous as well as crystalline phase of ZnSe. In addition the variation of the activation energy for conduction with frequency was studied in different region of temperature. The synthesized nanoparticles may be very useful for optoelectronic and electro optic device fabrications.

Acknowledgement

Authors would like to acknowledge to the Director, NPL for his continuous encouragement in pursuing the above studies. Authors are thankful to DST (impedance analysis were done using DST funded impedance analyzer).

References

[1] J. Ren, K. A. Bowers, B. Sneed, D. L. Dreifus, J.W. Cook, J. F. Schetzina, Appl. Phys. Lett. **57**, 1901 (1990).
[2] O. Schulz, M. Strassburg, T. Rissom, U. W. Pohl, D. Bimberg, Appl. Phys. Lett. **81**, 4916 (2002).
[3] P. Mahawela, G. Sivaraman, S. Jeedigunta, J. Gaduputi, M. Ramalingam, S. Subramanian, Mater. Sci. Eng. B **116**, 283 (2005).
[4] S. B. Mirov, V.V. Fedorov, K. Graham, I. S. Moskalev, V. V. Badikov, V. Panyutin, Opt. Lett. **27**, 909 (2002).
[5] H. R. Dobler, Appl. Opt. **28**, 455 (2003).
[6] N. Kouklin, L. Menon, A. Z. Wang, D.W. Thompson, J. A. Woollam, P. F. Williams, Appl. Phys. Lett. **79**, 4423 (2001).
[7] Y. Jing, X. M. Meng, W. C. Yiu, J. Liu, J. X. Ding, C. S. Lee, S. T. Lee, J. Phys. Chem. B **108**, 2784 (2004).
[8] D. V. Averin, A. N. Korokutov, K. K. Likharev, Phys. Rev. B **44**, 6199 (1991).
[9] R. D. Gould, C. J. Bowler, Thin Solid Films **164**, 281 (1988).
[10] B. B. Ismail, R. D. Gould, phys. stat. sol. (a) **115**, 237 (1989).
[11] S. Gogoi, K. Bagua, Thin Solid Films **92**, 227 (1982).
[12] R. Sathyamoorthy, S. K. Narayandass, C. Balasubramanian, D. Mangalaraj, Proc. Solid State Phys. Symp. **33C**, 409 (1991).
[13] Ireneusz Strzalkowski, Sharad Joshi, C. R. Crowell, Appl. Phys. Lett. **28**, 350 (1976).
[14] Mohd. Shakir, S. K. Kushwaha, K. K. Maurya, G. Bhagavannarayana, M. A. Wahab, Solid State commun. **149**, 2047 (2009).
[15] A. K. Jonscher, Dielectric Relaxation in Solids, Chelsea Dielectric Press, London (1983).
[16] A. J. Dekker. Solid State Physics, Englewood Cliff NJ, Prentice-Hall (1962).
[17] B. C. Choi, J. B. Kim, B. M. Jin, S. I. Yun, J. N. Kim. J. Korean Phys. Soc. **25**, 327 (1992).
[18] A. K. Jonscher, Universal Relaxation Law, Chelsea Dielectrics Press, London (1996).